Obesity-Linked Variants of Melanocortin-4 Receptor Are Misfolded in the Endoplasmic Reticulum and Can Be Rescued to the Cell Surface by a Chemical Chaperone

Susana Granell, Sameer Mohammad, Ramanagouda Ramanagoudr-Bhojappa, and Giulia Baldini

Department of Biochemistry and Molecular Biology, University of Arkansas for Medical Sciences, Little Rock, Arkansas 72205

Melanocortin-4 receptor (MC4R) is a G protein-coupled receptor expressed in the brain where it controls food intake. Many obesity-linked MC4R variants are poorly expressed at the plasma membrane and are retained intracellularly. We have studied the intracellular localization of four obesity-linked MC4R variants, P78L, R165W, I316S, and I317T, in immortalized neurons. We find that these variants are all retained in the endoplasmic reticulum (ER), are ubiquitinated to a greater extent than the wild-type (wt) receptor, and induce ER stress with increased levels of ER chaperones as compared with wt-MC4R and appearance of CCAAT/enhancer-binding protein homologous protein (CHOP). Expression of the X-box-binding-protein-1 (XBP-1) with selective activation of a protective branch of the unfolded protein response did not have any effect on the cell surface expression of MC4R-I316S. Conversely, the pharmacological chaperone 4-phenyl butyric acid (PBA) increased the cell surface expression of wt-MC4R, MC4R-I316S, and I317T by more than 40%. PBA decreased ubiquitination of MC4R-I316S and prevented ER stress induced by expression of the mutant, suggesting that the drug functions to promote MC4R folding. MC4R-I316S rescued to the cell surface is functional, with a 52% increase in agonist-induced cAMP production, as compared with untreated cells. Also direct inhibition of wt-MC4R and MC4R-I316S ubiquitination by a specific inhibitor of the ubiquitin-activating enzyme 1 increased by approximately 40% the expression of the receptors at the cell surface, and the effects of PBA and ubiquitin-activating enzyme 1 were additive. These data offer a cell-based rationale that drugs that improve MC4R folding or decrease ER-associated degradation of the receptor may function to treat some forms of hereditary obesity. **(*Molecular Endocrinology* 24: 1805–1821, 2010)**

The brain integrates different signals from the periphery such as metabolites and hormones to control food intake. Central to this pathway is the function of melanocortin-4 receptor (MC4R), which belongs to the family of seven *trans*-membrane G protein-coupled receptors (GPCRs). MC4R knockout mice are obese (1) and so are humans with naturally occurring mutations of MC4R (2). Although MC4R is expressed in many areas of the brain, control of food intake occurs at specialized sites. In this respect, it has been shown that restoration of MC4R expression in the hypothalamic paraventricular nucleus and in the amygdala of mice that do not express MC4R prevents 60% of the obesity (3). In the paraventricular nuclei of the hypothalamus, MC4R responds to an agonist,

ISSN Print 0888-8809 ISSN Online 1944-9917
Printed in U.S.A.

doi: 10.1210/me.2010-0071 Received February 25, 2010. Accepted June 8, 2010.
First Published Online July 14, 2010

Abbreviations: ABTS, 2,2′-azino-bis(3-ethylbenzthiazoline-6-sulfonic acid; ATF6, activating transcription factor-6; CHOP, CCAAT/enhance-binding protein homologous protein; CFTR, ΔF508 cystic fibrosis transmembrane conductance regulator; ER, endoplasmic reticulum; ERAD, ER-associated degradation; GFP, green fluorescent protein; GPCR, G protein-coupled receptor; GRP, glucose-regulated protein; IRE1, inositol-requiring protein-1; HA, hemagglutinin; MC4R, melanocortin-4 receptor; PBA, 4-phenyl butyric acid; PERK, protein kinase RNA-like ER kinase; POD, peroxidase; UBE1-41, the inhibitor of ubiquitin-activating enzyme 1; V2R, vasopressin type-2 receptor; wt, wild type; XBP-1, X-box-binding-protein-1.

α-MSH, and to an antagonist, agouti-related protein, which compete with each other for binding to MC4R. MC4R binding to α-MSH leads to stimulation of the receptor activity with activation of adenylate cyclase-dependent production of cAMP. Two decades ago, pioneering work reported the first cases of severe obesity and hyperphagia caused by *MC4R* mutations (4, 5). Since then, many studies have found association between *MC4R* variants and inherited and early-onset obesity (2, 6–10). More recent studies have found prevalence of *MC4R* mutations in early-onset obesity (2.83%) (11) as well as in severely obese adults (2.25%) (12). It has been found that most of the obesity-linked MC4R variants have defective cell surface expression of the receptor with MC4R retention in an intracellular localization (6, 13–15). Pharmacological studies indicate that some of the obesity-linked MC4R variants that are retained intracellularly have normal responsiveness to α-MSH, whereas other variants have moderately reduced or severely reduced response to the hormone (11, 14). It is possible that some mutations lead only to minor changes in the structure and function of the receptor. Consequently, rescue of cell surface expression of the mutated receptor may be a possible approach to treat some forms of inherited obesity. In this respect, although intracellular retention of obesity-linked MC4R variants is well documented, the cell location where the variants are retained and the mechanism by which this retention occurs have not yet been explored. Here we have selected four obesity-linked MC4R variants, P78L, R165W, I316S, and I317T (6, 13, 15–17), which are retained intracellularly, to study their cell localization and mechanism of reduced plasma membrane expression. These mutations occur at different sites of the protein, namely the second transmembrane domain (P78L), the second intracellular domain (R165W), and the C-terminal domain (I316S and I317T), with one of them (P78L) having no detectable stimulation by α-MSH, two others with decreased potency for the hormone (R165W and I316S) and one with similar potency (I317T) (14). We find that all of them lead to the receptor being trapped in the endoplasmic reticulum (ER) as a ubiquitinated protein, indicating that step as a possible therapeutic target for some forms of inherited obesity.

Results

Obesity-linked MC4R variants are retained in the ER

To determine the amount of obesity-linked MC4R variants expressed at the plasma membrane neuroblastoma Neuro2A (N2A) cells were transiently transfected with tagged wild-type (wt)-HA-MC4R-GFP and mutated HA-MC4R-GFP (P78L, R165W, I316S, and I317T). The amount of receptor at the cell surface was measured by using an immunoassay that detects the hemagglutinin (HA) tag placed at the extracellular N terminus of the protein by using anti-HA antibody coupled to peroxidase (POD) (18). The amount of mutated HA-MC4R-GFP expressed at the cell surface of N2A cells was less than 50% of that of the wt receptor (Fig. 1A), consistent with the data obtained by others in human embryonic kidney (HEK) 293 cells (13, 14). To visualize the cell distribution of wt and mutated receptor, cells transfected with wt-HA-MC4R-GFP and mutated HA-MC4R-GFP-I316S and I317T were stained with anti-HA antibody and secondary antibody coupled to Cy3. The I316S and I317T variants were expressed at the plasma membrane less abundantly than the wt receptor (Fig. 1B, Cy3), consistent with the immunoassay data. The entire population of wt-HA-MC4R-GFP receptor, visualized by green fluorescent protein (GFP) fluorescence localized to the plasma membrane and to a perinuclear endosomal compartment (Fig. 1B, GFP). Conversely, the I316S and I317T mutants had a more diffuse, reticular distribution.

MC4R localizes to the plasma membrane and in endosomes and recycles constitutively (18). When N2A cells transiently transfected with wt-HA-MC4R-GFP are incubated at 37 C in the presence of anti-HA antibody, the antibody binds to the entire pool of receptors that traffics between the plasma membrane and the endosomal compartment. This pool of recycling receptors can then be visualized by staining fixed and permeabilized cells with secondary antibodies conjugated to Cy3 (Fig. 1C). Because the GFP tag attached to MC4R visualizes the entire pool of cell receptors, the extent by which the GFP and Cy3 fluorescence overlap, is a measure of the fraction of total MC4R that is either at the plasma membrane or in the endosomal compartment. In the case of wt-HA-MC4R-GFP, there was extensive overlap between GFP and Cy3 fluorescence (Fig. 1, C and D), indicating that most of wt receptor expressed in the cell is either localized at the plasma membrane or in endosomes. Conversely, in the case of HA-MC4R-GFP-I316S and -I317T, most of the GFP did not colocalize with Cy3 (Fig. 1, C and D), indicating that only a minor fraction of the total population of mutated MC4R is found either at the plasma membrane or in the endosomal compartment.

The rate of internalization of wt-HA-MC4R-GFP and mutated HA-MC4R-GFP-I316S and I317T from the cell surface was the same (Fig. 1E). This suggests that, once deployed to the plasma membrane, wt and mutated MC4R are endocytosed by the same kinetics. To determine whether traffic along the recycling compartment was unaffected, we measured the rate of externalization

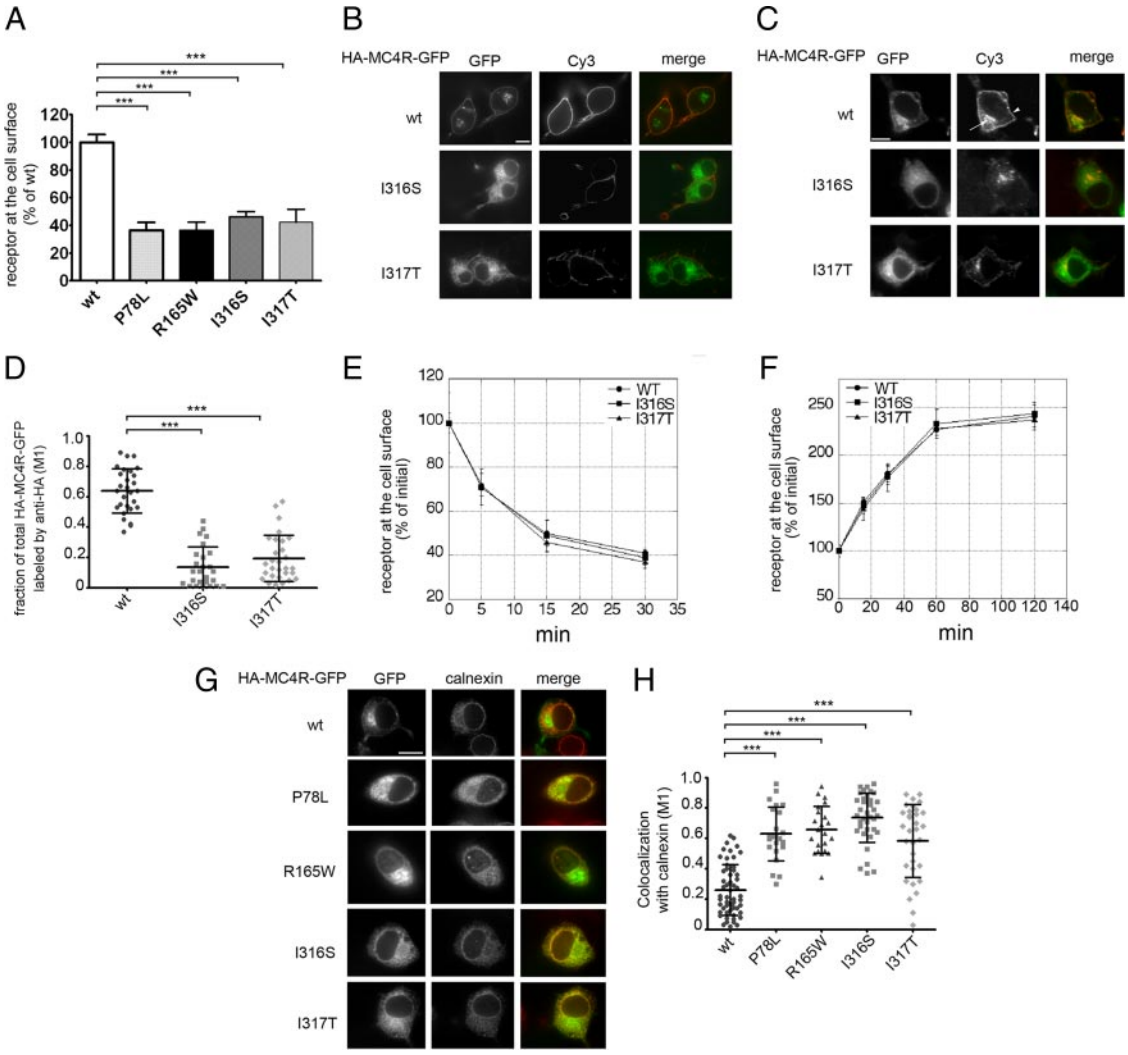

FIG. 1. Obesity-linked MC4R mutants are retained in the ER. A, N2A cells were transiently transfected with wt-HA-MC4R-GFP and mutated HA-MC4R-GFP (P78L, R165W, I316S, and I317T). HA-MC4R-GFP at the cell surface was measured by ELISA. Data are expressed as percentage of the wt receptor. B, Cells were transfected with wt-HA-MC4R-GFP and mutated HA-MC4R-GFP (I316S and I317T), transferred at 4 C, incubated with primary rat monoclonal anti-HA antibodies, fixed, and incubated with secondary Cy3-conjugated antirat antibodies. C, N2A cells were transfected as in B. Cells were incubated with rat anti-HA antibodies for 2 h at 37 C. Cells were fixed, washed with PBS, permeabilized, and incubated with Cy3-conjugated antirat antibodies. *Arrow* and *arrowhead* indicate endosomal compartment and plasma membrane, respectively. D, Quantification of the confocal images of the experiment shown in C. The wt-HA-MC4R-GFP (n = 30) and mutated HA-MC4R-GFP (I316S n = 31, I317T n = 30), M1, Mander's overlap coefficient. E and F, N2A cells were transfected with wt-HA-MC4R-GFP and mutated HA-MC4R-GFP (I316S and I317S). Receptor internalization (E) and exocytosis (F) were measured as previously reported (18). G, N2A cells were transiently transfected with wt-HA-MC4R-GFP and mutant HA-MC4R-GFP (P78L, R165W, I316S, and I317T). Cells were permeabilized and stained with primary rabbit polyclonal anti-calnexin and secondary Cy3-conjugated antirabbit antibodies. H, Quantification of the colocalization of MC4R with calnexin was done using cells transfected with wt-HA-MC4R-GFP (n = 55) and mutated HA-MC4R-GFP (P78L n = 23, R165W n = 22, I316S n = 36, I317T n = 33). *Bars*, 25 μm. ***, $P < 0.0001$.

of wt-HA-MC4R-GFP (18) and the HA-MC4R-GFP-I316S and HA-MC4R-GFP-I317T mutants in the presence of cycloheximide to block protein synthesis (Fig. 1F). Again, it appeared that the kinetics of receptor externalization were the same in the case of the wt and mutated receptors, indicating that traffic across the recycling pathway is unchanged by the mutations.

The diffuse, reticular distribution of the MC4R-I316S and -I317T variants, together with the absence of kinetic defects along the recycling pathway, suggested that reduced expression of the mutants at the plasma membrane is due to defects along the biosynthetic pathway. To determine whether this was the case, cells expressing wt-HA-MC4R-GFP and mutated HA-MC4R-GFP (P78L, R165W, I316S, and I317T) were costained with antibodies against the ER resident protein calnexin (Fig. 1G). Quantitative analysis revealed that all mutated HA-MC4R-GFP have significantly increased colocalization with calnexin as compared with that of wt-HA-MC4R-GFP (Fig. 1, G and H). This was true also for HA-MC4R-I316S and -I317T that do not have the GFP tag (Supplemental Fig. 1, published on The Endocrine Society's Journals Online web site at http://mend.endojournals.org). These data indicate that obesity-

linked variants of MC4R lead to increased retention of the receptor in the ER.

MC4R bearing obesity-linked mutations have greater tendency than wt-MC4R to be ubiquitinated

Proteins that enter the biosynthetic pathway in the ER and fail to fold are recognized by a quality control system and targeted to the ER-associated degradation (ERAD) pathway by ubiquitination (19). A standard method to detect ubiquitinated GPCR is coexpression with tagged ubiquitin, immunoprecipitation of the GPCR, and immunoblot with antibodies against the tag (20). To test the possibility that the MC4R mutants are prone to ubiquitination, N2A cells were cotransfected with Flag-ubiquitin and either wt or mutated HA-MC4R-GFP, and the cell lysates were immunoprecipitated with the anti-HA antibody. The wt-HA-MC4R-GFP from the cell lysates appeared by Western blot analysis as multiple bands with a more prominent one migrating at 78 kDa in the 9% SDS-PAGE (Fig. 2A, *lower arrowhead*), close to the predicted molecular mass of 66 kDa (~37 kDa HA-MC4R + ~30 kDa of the GFP) and as another band at 250 kDa (Fig. 2A, *upper arrowhead*). In addition, there were also multiple HA-MC4R-GFP bands at intermediate molecular mass between 78 and 250 kDa (Fig. 2A, *vertical bar*). All HA-MC4R-GFP proteins bearing the obesity-linked mutations migrated predominantly as intermediate and high molecular mass species, with reduced immunoreactivity of the band at 78 kDa (Fig. 2A, *lower arrowhead*). When immunoprecipitated samples were separated by a 7% SDS-PAGE and analyzed by Western blot with anti-HA antibody, wt-HA-MC4R-GFP appeared as a prominent band at 78 kDa (Fig. 2C, *arrow*) and a faint smear at higher molecular mass (Fig. 2C, *vertical bar*). Differently, all mutated HA-MC4R-GFP migrated predominantly as intermediate and high molecular mass bands with almost undetectable immunoreactivity at 78 kDa (Fig. 2C, *vertical bar*). When the immunoprecipitated HA-MC4R-GFP was analyzed with the anti-Flag antibody, ubiquitin was found associated with both wt and mutated receptors and appeared as a smear between 98 and 250 kDa (Fig. 2D). Samples immunoprecipitated from cells transfected with mutated HA-MC4R-GFP exhibited more ubiquitin immunoreactivity than the sample immunoprecipitated from cells transfected with wt-HA-MC4R-GFP (Fig. 2D). Thus, it appears that a larger fraction of mutated than of wt-HA-MC4R-GFP is ubiquitinated, consistent with the shift in molecular mass observed in the cell lysates (Fig. 2A). To determine whether ubiquitination of the wt and mutated receptors was caused by the GFP tag, the experiment was repeated using cells cotransfected with wt-HA-MC4R and HA-MC4R-I316S and Flag-ubiquitin (Supplemental Fig. 2) with similar results. In conclusion, the experiments of Fig. 2 indicate that mutated MC4R have a greater tendency to be ubiquitinated than wt-MC4R. These observations suggest that these proteins exist as misfolded species targeted for degradation by ERAD.

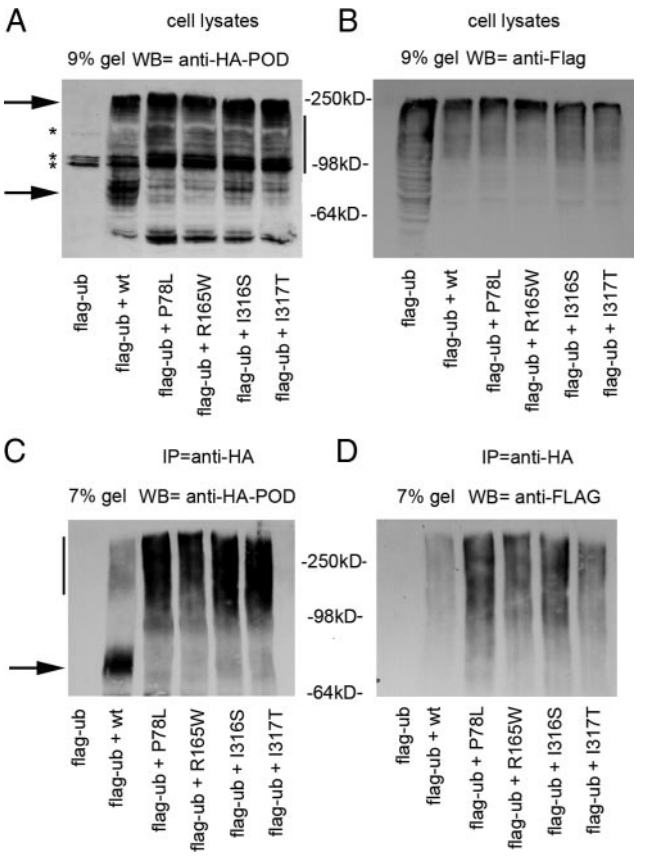

FIG. 2. More of HA-MC4R-GFP bearing obesity-linked mutations than of wt receptor is ubiquitinated. A and B, N2A cells were transiently transfected with Flag-ubiquitin (Flag-ub) or cotransfected with Flag-ubiquitin and wt-HA-MC4R-GFP or mutated HA-MC4R-GFP (P78L, R165W, I316S, and I317T). Cell lysates were analyzed by Western blot (WB) by using the indicated antibodies. C and D, Immunoprecipitations (IP) from cell lysates were carried out with anti-HA antibodies and analyzed by Western blot by using the indicated antibodies. *Arrows* indicate the bands at 250 and 78 kDa. Vertical bar indicate MC4R immunoreactivity between 78 and 250 kDa. *, Unspecific bands.

Expression of obesity-linked MC4R variants causes ER stress

When unfolded proteins accumulate in the ER, this causes ER stress (21). The unfolded protein response (UPR) is a complex signaling pathway that leads to increased synthesis of chaperones such as the glucose-regulated proteins (GRPs) GRP78 and GRP94, which assist in protein folding, and of the proapoptotic transcription factor CCAAT/enhancer-binding protein homologous protein (CHOP) (22). If obesity-linked MC4R variants had a greater tendency to misfold than wt-MC4R, then expression of these proteins may induce the UPR with an in-

crease of ER chaperones and CHOP. KDEL is a C-terminal signal sequence required for residency of many proteins that are to be retained in the ER, including the ER chaperones GRP78 and GRP94 (23). Western blot analysis using anti-KDEL antibody showed that N2A cells expressing mutated HA-MC4R-GFP had increased levels of GRP78 and GRP94 as compared with the wt receptor (Fig. 3, A and B). It is possible that some of the effects of the obesity-linked MC4R variants on ER stress could be mediated by protein overload in the ER in the transiently transfected cells. To explore this possibility, we selected, by immunofluorescence microscopy, popu-

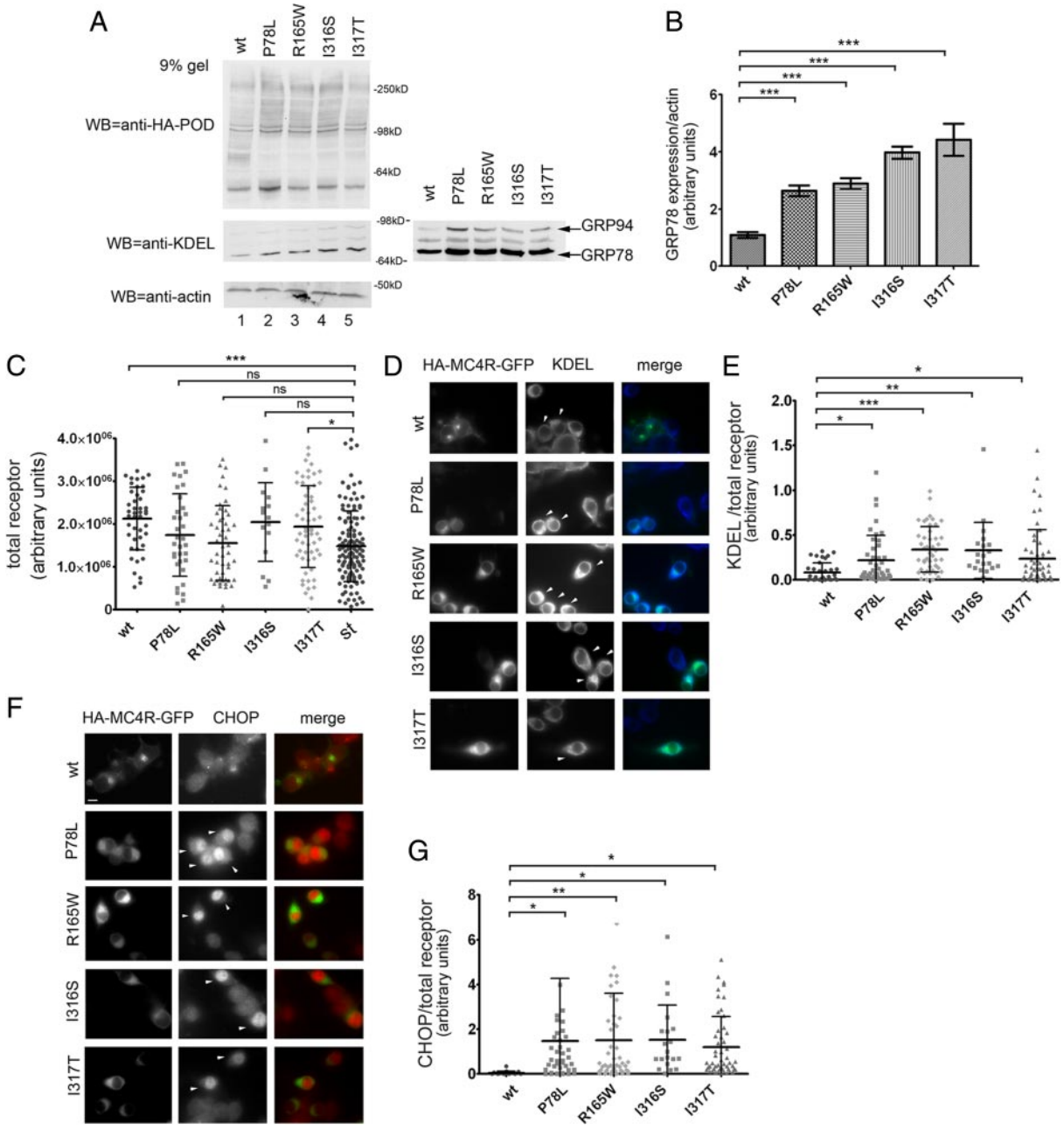

FIG. 3. Expression of mutated HA-MC4R-GFP-P78L, -R165W, -I316S, and I317T induces ER stress. A, N2A cell lysates were derived from cells transiently transfected with wt-HA-MC4R-GFP and mutated HA-MC4R-GFP (P78L, R165W, I316S, and I317T). Cell lysates were analyzed by Western blot with the indicated antibodies. The *panel on the right* shows a more exposed blot from another experiment. B, GRP78 and actin levels were measured by densitometry. Averages and SD were determined from three independent experiments including those shown in A. C, N2A cells were transfected as in A. GFP fluorescence of cells transiently transfected with wt-HA-MC4R-GFP (n = 44) and mutated HA-MC4R-GFP (P78L n = 44, R165W n = 50, I316S n = 20, and I317T n = 60) are compared with the stable clone of wt-HA-MC4R-GFP (n = 132) (st). D and F, Cell immunostaining was done using mouse monoclonal anti-KDEL antibodies and rabbit polyclonal anti-CHOP antibodies. Secondary staining was carried out using Cy5-conjugated antimouse antibodies and Cy3-conjugated antirabbit antibodies, respectively. *Arrowheads* indicate transfected cells. E, Averages and SD of KDEL pixel intensity normalized to HA-MC4R-GFP content from the cell population analyzed in C. G, Averages and sd of CHOP pixel intensity normalized to HA-MC4R-GFP content from the cell population analyzed in C. *Bar*, 25 μm. *, $P < 0.05$; **, $P < 0.001$; ***, $P < 0.0001$; and ns (nonsignificant), $P > 0.05$.

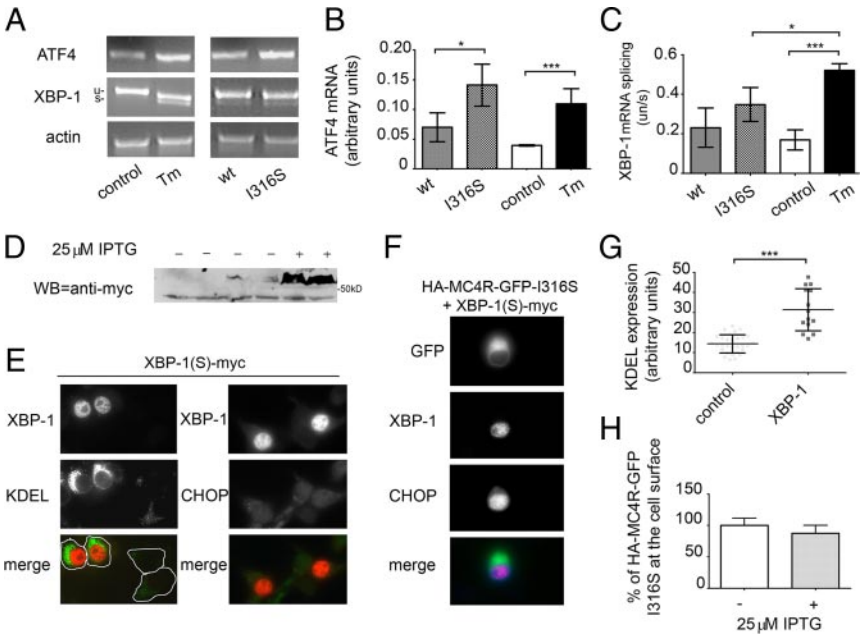

FIG. 4. Induction of a protective branch of the UPR does not increase cell surface expression of mutated HA-MC4R-GFP-I316S. A, *Left panel*, N2A cells were left untreated (control) or treated with 16 h with tunicamycin (Tm); *right panel*, N2A cells were transiently transfected with wt-HA-MC4R-GFP and mutated HA-MC4R-GFP-I316S. Spliced XBP-1 and ATF4 mRNA induction was measured by RT-PCR. B and C, Quantification of ATF4 mRNA (B) and of spliced XBP-1 mRNA (expressed by the ratio of unspliced XBP-1 mRNA to spliced XBP-1 mRNA) (C) was done by band densitometry from three different experiments including the gel shown in A. D, Induction of spliced, Myc-tagged XBP-1 (S) [XBP-1(S)-myc] expression was analyzed by Western blot using the rabbit polyclonal anti-myc antibodies. E, N2A cells were transfected as indicated and immunostained by using either mouse monoclonal anti-KDEL and rabbit polyclonal anti-myc antibodies (*left panel*) or rabbit polyclonal anti-CHOP antibodies and mouse monoclonal anti-myc (*right panel*). Secondary staining was carried out using Cy3-conjugated antirabbit and fluorescein isothiocyanate (FITC)-conjugated antimouse antibodies (*right panel*) and FITC-conjugated antirabbit and Cy3-conjugated antimouse antibodies (*left panel*). F, Cells transfected with XBP-1(S)-myc were immunostained by using mouse monoclonal anti-myc and rabbit polyclonal anti-CHOP antibodies. Secondary staining was carried out using Cy5-conjugated antirabbit and Cy3-conjugated antimouse antibodies. G, Averages and SD of KDEL pixel intensity of untransfected cells (control, n = 25) and cells expressing XBP-1(S)-myc (n = 15). H, N2A cells were transiently transfected with XBP-1(S)-myc-ptune and mutated HA-MC4R-GFP-I316S in the absence or presence of 25 μM isopropyl β-D-1-thiogalactopyranoside (IPTG). MC4R at the cell surface was measured by a spectrophotometric assay as in Fig. 1A. *Bar*, 25 μm. *, $P < 0.05$; ***, $P < 0.0001$.

lations of cells transiently expressing the receptor at the same level (HA-MC4R-GFP-P78L, -R165W, and -I316S) or at similar levels (wt-HA-MC4R-GFP and HA-MC4R-GFP-I317T, less than 40% increase) as that of a stably transfected clone of N2A cells expressing wt-HA-MC4R-GFP (Fig. 3C). In this stably transfected clone, the exogenous receptor (HA-MC4R-GFP) increases only by 30% the total amount of MC4R expressed by the cell (18). In the selected population of cells transiently expressing low levels of exogenous receptor, expression of mutated HA-MC4R-GFP increased by 2-fold KDEL immunoreactivity as compared with wt-HA-MC4R-GFP [Fig. 3, D (*arrowheads*) and E]. In the same population of cells, mutated HA-MC4R-GFP induced CHOP expression in the nucleus [Fig. 3, F (*arrowheads*) and G]. Together, the findings of Fig. 3 suggest that obesity-linked MC4R variants, even when expressed at levels comparable with that of the endogenous receptor, induce ER stress. This is consistent with the concept that the MC4R variants have a tendency to misfold.

Induction of a protective branch of the UPR does not improve cell surface expression of HA-MC4R-GFP-I316S

The UPR consists of a set of three signaling pathways: protein kinase RNA-like ER kinase (PERK), activating transcription factor-6 (ATF6) and inositol-requiring protein-1 (IRE1) (22, 24). Of these signaling pathways, both IRE1 and ATF6 induce a protective response with an increase of ER chaperones involved in protein folding and ERAD, whereas the PERK pathway induces expression of proapoptotic factors such as CHOP (22). It has also been reported that in the presence of persistent ER stress, IRE1 and ATF6 pathways are reduced, whereas the PERK pathway is maintained (25). The IRE1 pathway leads to splicing of X-box-binding protein 1 (XBP-1) mRNA into an active transcription factor that translocates to the nucleus to regulate expression of many cell chaperones including GRP78 and GRP94 (22, 26, 27). Differently, the PERK pathway leads to increased levels of ATF4, another transcription factor, which up-regulates CHOP (22). When N2A cells were exposed for 16 h to tunicamycin, which induces ER stress by inhibiting N-linked glycosylation and protein folding, ATF4 mRNA (Fig. 4, A and B) and spliced XBP-1 mRNA (Fig. 4, A and C) were both increased as compared with untreated cells, indicating that both the PERK and the IRE1 pathways, respectively, are activated. In contrast, at 48 h after transfection, in cells expressing HA-MC4R-GFP-I316S spliced XBP-1 mRNA was unchanged (Fig. 4, A and C), whereas ATF4 mRNA was increased as compared with cells expressing wt-HA-MC4R-GFP (Fig. 4, B and C). These data suggest that expression of HA-MC4R-GFP-I316S leads to full activation of the proapoptotic branch of the UPR and to an attenuated response of a protective branch of the pathway. It has been found that artificial expression of active,

spliced XBP-1 protects cells from sustained ER stress perhaps by maintaining an elevated folding capacity of the ER (25). Thus, expression of spliced XBP-1, by expanding the ER capacity, could help folding of mutated MC4R and promote expression of the protein at the cell surface. When spliced XBP-1 was expressed in N2A cells (Fig. 4D), there was selective activation of the protective branch of the UPR, as indicated by increased levels of KDEL immunoreactivity [Fig. 4, E (*left panel*) and G], although CHOP was not induced (Fig. 4E, *right panel*). This indicates that the protective and not the proapoptotic branch of the UPR is activated by expression of spliced XBP-1. However, in cells expressing spliced XBP-1 together with HA-MC4R-GFP-I316S, CHOP activation was still induced (Fig. 4F), indicating unresolved ER stress. In addition, expression of the active transcription factor did not increase the level of HA-MC4R-GFP-I316S localized at the plasma membrane (Fig. 4H). In conclusion, the data of Figs. 3 and 4 indicate that expression of obesity-linked MC4R variants already induces the UPR and that modulation of this pathway to promote protective responses does not resolve misfolding of mutated MC4R.

4-Phenyl butyric acid (PBA) rescues cell surface expression of obesity-linked MC4R variants and increases cAMP production in response to agonist stimulation

Incubation with a chemical chaperone, PBA, has been shown to improve secretion of mutated proteins retained in the ER. For example, incubation with PBA increases secretion of a mutated α-1 antitrypsin in a murine hepatoma cell line where the protein is retained in the ER and inclusion bodies (28). Incubation with PBA also increases secretion of mutated human preproparathyroid hormone that is retained in the ER and induces ER stress (29). PBA has also been reported to improve trafficking of ΔF508 cystic fibrosis transmembrane conductance regulator (CFTR) mutant from the ER to the plasma membrane (30). Differently, PBA did not promote exit from the ER of some GPCR such as disease-linked rhodopsin and vasopressin type-2 receptor (V2R) mutants (31, 32). It appears that although PBA has a general effect on the ability of the ER to respond to stress perhaps by up-regulating heat-shock proteins involved in protein folding, this is not applicable to all proteins that misfold in the ER (33). To test whether PBA promotes folding and cell surface expression of obesity-linked MC4R variants, N2A cells transfected with wt-HA-MC4R-GFP and mutated HA-MC4R-GFP were incubated with or without PBA for 24 and 48 h. Treatment with PBA for 24 h increased by 40 $\pm$ 21% the amount of the mutated HA-MC4R-GFP-I316S at the cell surface (Fig. 5A), whereas wt-HA-MC4R-GFP and HA-MC4R-GFP-P78L, -R165W, and -I317T mutants remained unchanged. After 48 h treatment, the amount of receptor to the cell surface of wt-HA-MC4R-GFP was increased by 70.4 $\pm$ 18.4%, HA-MC4R-GFP-P78L by 24.3 $\pm$ 6.5%, HA-MC4R-GFP-I316S by 47.9 $\pm$ 15.2%, and HA-MC4R-GFP-I317T by 41.3 $\pm$ 21.0% (Fig. 5B). Conversely, incubation with the PBA did not increase cell surface expression of HA-MC4R-GFP-R165W, indicating that the drug can selectively rescue to the plasma membrane wt-MC4R, and most, but not all, of obesity-linked MC4R variants retained in the ER and does so to different degrees. To determine whether PBA increased the fraction of total cell receptor that reaches the plasma membrane, we carried out immunofluorescence microscopy. When unpermeabilized cells transfected with HA-MC4R-GFP and treated with or without PBA were incubated in the presence of anti-HA antibody to label the population of receptors at the cell surface (Cy3) (Fig. 5C), the ratio of Cy3 fluorescence (receptor at the plasma membrane) to GFP fluorescence (total receptor monitored by the GFP tag) was increased by approximately 2-fold by PBA (Fig. 5D). In cells treated with the drug, the GFP fluorescence appeared less diffuse, with a more evident plasma membrane staining (Fig. 5C, GFP, *arrowhead*) and punctuated endosomal compartment (Fig. 5C, GFP, *arrows*). This indicated that PBA increases the fraction of total cell receptor that traverses the biosynthetic pathway to reach the plasma membrane and cycles to the endosomes. The GT1-7 cell line is derived from murine hypothalamic neurons and expresses endogenous MC4R (34). Similarly to N2A cells, treatment of immortalized hypothalamic GT1-7 neurons expressing HA-MC4R-GFP-I316S with PBA increased the cell surface expression of the receptor by 70% (Fig. 5E).

Most of the obese individuals carrying disease-associated MC4R variants are heterozygous. It is likely that in these individuals loss of total receptor number expressed at the plasma membrane is the cause of the disease (7). Such loss may result from a decreased number of mutated receptors reaching the plasma membrane as well as a dominant negative effect induced by interactions of the wt receptor with the mutated receptor with consequent further decrease of functional receptor at the plasma membrane. When wt-HA-MC4R-GFP was coexpressed with Myc-MC4R-GFP-I316S or Myc-MC4R-GFP-I317T, the amount of wt receptor detected at the cell surface by the immunoassay with the anti-HA antibody was decreased as compared with cells that were cotransfected with wt-Myc-MC4R-GFP (Fig. 5F). Thus, expression of MC4R bearing obesity-linked mutations impairs cell surface localization of coexpressed wt-MC4R. In the cotransfection assay, incubation with PBA increased to similar levels

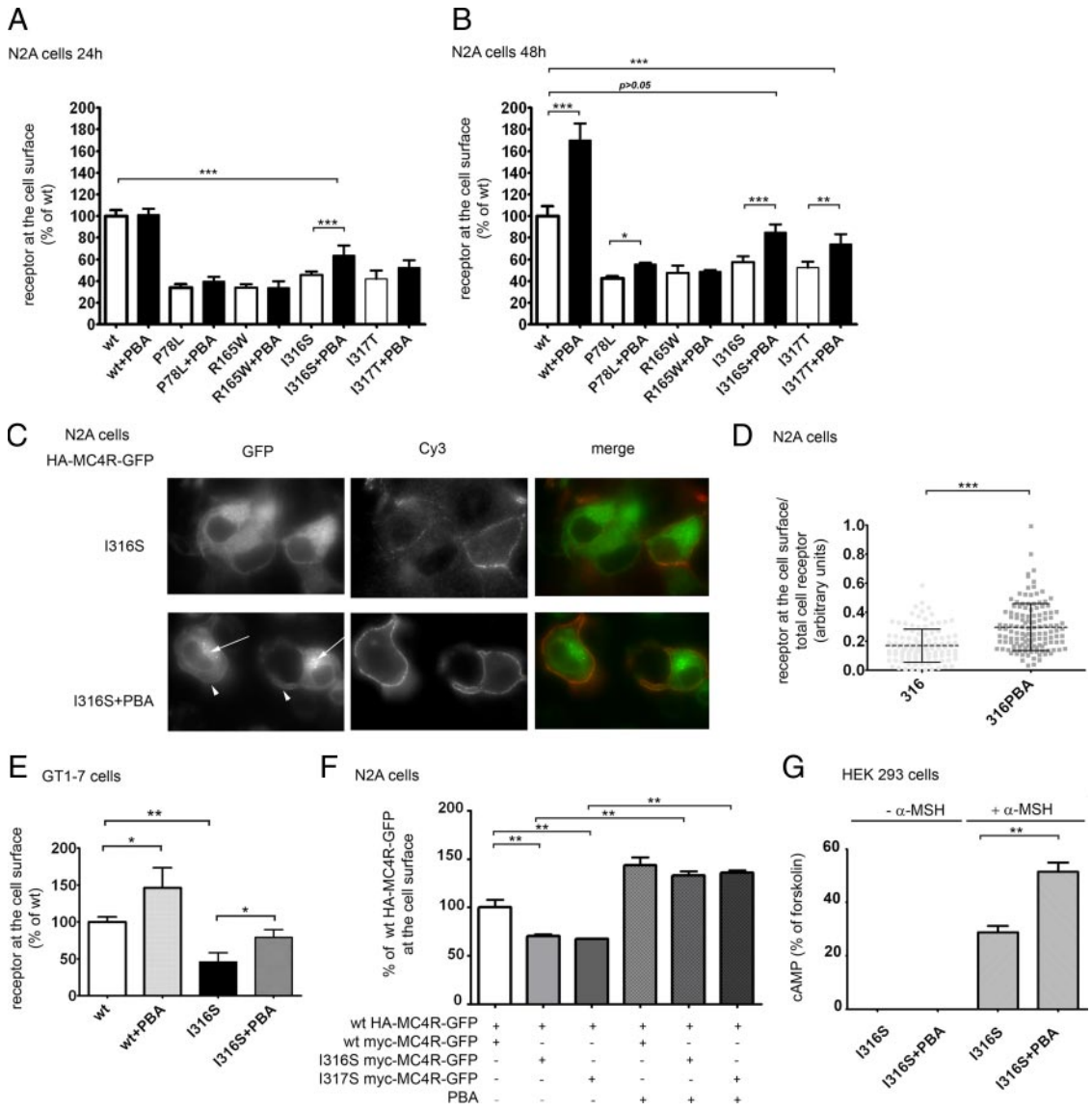

FIG. 5. PBA increases cell surface expression and signaling of mutated HA-MC4R-GFP-I316S. A and B, N2A cells were transiently transfected with wt-HA-MC4R-GFP and mutated HA-MC4R-GFP (P78L, R165W, I316S, and I317T) and treated with vehicle alone or 2 mM PBA for 24 h (A) or 48 h (B). HA-MC4R-GFP at the cell surface was measured by a spectrophotometric assay as in Fig. 1A. C, N2A cells were transiently transfected with mutated HA-MC4R-GFP-I316S and treated with vehicle alone (I316S) or 2 mM PBA (I316S+PBA). Cells were transferred at 4 C, incubated with rat monoclonal anti-HA primary antibodies, fixed, and incubated with Cy3-conjugated antirat antibodies. D, Quantification of the experiment in C (I316S n = 116, I316S+PBA n = 131). E, GT1-7 cells were transiently transfected with wt-HA-MC4R-GFP and mutated HA-MC4R-GFP-I316S and treated with vehicle alone or 2 mM PBA for 48 h. MC4R at the cell surface was measured as in A. F, N2A cells were transiently transfected as indicated and treated with vehicle alone or 2 mM PBA for 48 h. HA-MC4R-GFP at the cell surface was measured as in A. G, HEK 293 cells were transiently transfected with mutated HA-MC4R-GFP-I316S and treated with vehicle alone (I316S) or 2 mM PBA for 48 h (I316S+PBA). Cells were stimulated with 100 nM α-MSH or with 10 μM forskolin for 15 min at 37 C. The amount of cAMP generated by cells incubated with and without α-MSH was expressed as percentage of that induced by incubation with forskolin. *Bar*, 25 μm. *, $P < 0.05$; **, $P < 0.001$; ***, $P < 0.0001$.

the localization of wt-HA-MC4R-GFP at the cell surface in the case where the protein was coexpressed with either the wt or mutated receptors. This indicates that PBA promotes cell surface expression of wt-MC4R when the receptor is coexpressed with mutated MC4R.

It has been reported that most obesity-linked variants, including MC4R bearing the I316S mutation respond to endogenous α-MSH, albeit with reduced potency (14). It is possible that PBA-induced increase of HA-MC4R-GFP-I316S at the plasma membrane leads to increased signaling of the receptor. N2A cells express endogenous MC4R (18), which makes it difficult to monitor the activity of the exogenous receptor above background. When HEK 293 cells expressing HA-MC4R-GFP-I316S were treated with α-MSH, the intracellular cAMP increased by more than 10-fold to 28.8 ± 4.2% of the level obtained by maximal adenylate cyclase stimulation with forskolin (Fig. 5G). Incubation with PBA further increased the level of cAMP production in response to α-MSH by 51.5 ± 4.8% as compared with untreated cells, consistent with the in-

creased levels of receptor at the plasma membrane in response to the drug. In conclusion, it appears that PBA-induced rescue of mutated MC4R-I316S localization at the cell surface expression leads to increased activity in response to agonist stimulation.

PBA increases cell surface expression of MC4R by promoting folding of the protein

We reasoned that the extent by which mutated MC4R is ubiquitinated could be used as an assay to determine whether PBA-dependent enhancement of cell surface localization and function of HA-MC4R-GFP-I316S is due to increased folding of the receptor. When cells were cotransfected with wt and mutated HA-MC4R-GFP-I316S and with Flag-ubiquitin, and receptors were immunoprecipitated, it appeared that PBA increased expression of the 78-kDa species of both wt-HA-MC4R-GFP and HA-MC4R-GFP-I316S (Fig. 6A, *arrowhead*), suggesting that a more abundant population of these proteins exists as mature forms. Western blot analysis of the immunoprecipitated samples with the anti-Flag antibody showed that the wt and mutated HA-MC4R-GFP were less ubiquitinated when cells were incubated with PBA (Fig. 6B). This suggests that PBA improves folding of both wt-MC4R and MC4R-I316S, thereby causing indirect inhibition of receptor ubiquitination. We have found that, unlike wt-MC4R and MC4R-I316S, MC4R-R165W was not rescued to the cell surface by treatment with PBA, suggesting that the protein remains misfolded (Fig. 5, A and B). PBA did not decrease ubiquitination of HA-MC4R-GFP-R165W (Fig. 6C), indicating that indeed this receptor remains misfolded and is targeted for degradation.

It appears that a fraction of both wt and mutated receptor remains misfolded in the ER and is targeted for degradation by the ubiquitination machinery. Therefore, it is possible that direct inhibition of ubiquitination itself may decrease ERAD of MC4R, thereby increasing the fraction of receptor able to fold and to reach the plasma membrane. To test this possibility, we treated cells with a specific inhibitor of the ubiquitin-activating enzyme 1 (UBE1-41) (35). When cells were cotransfected with HA-MC4R-GFP-I316S and Flag-ubiquitin and the receptor was immunoprecipitated with anti-HA antibodies, receptor-associated Flag immunoreactivity was decreased by incubation with UBE1-41 (Fig. 6E). This indicates that UBE1-41 inhibited ubiquitination of the receptor. Incubation with the inhibitor increased the expression of wt-HA-MC4R-GFP by 54.0 ± 7.15% and of HA-MC4R-GFP-I316S by 38.8 ± 20% at the plasma membrane (Fig. 6D). Moreover, the combined effects of PBA and UBE1-41 increased surface expression of wt-HA-MC4R-GFP by 105.2 ± 30.9% and of HA-MC4R-GFP-I316S by 89.5 ± 29.61% (Fig. 6D). This additive effect suggests that these drugs function at different steps along the pathway of MC4R maturation, with PBA improving folding of MC4R and inhibitors of the ubiquitination machinery decreasing ERAD of the receptor. Importantly, incubation with both PBA and UBE1-41 increased cell surface expression of HA-MC4R-GFP-I316S to the same level as wt-HA-MC4R-GFP in untreated cells. Incubation with UBE1-41 did not increase expression of mutated HA-MC4R-GFP-P78L and R165W at the plasma membrane (Fig. 6F). These experiments, together with the observation that PBA did not decrease the extent by which HA-MC4R-GFP-R165W is targeted for degradation by ubiquitin, suggest that the MC4R-R165W variant is misfolded beyond repair.

We have found that expression of disease-linked MC4R variants and not of wt-MC4R induced ER stress with increased levels of ER chaperones and of CHOP, indicating that these proteins are misfolded. When cells expressing wt-HA-MC4R-GFP were treated with PBA, the level of GRP78 expression did not change (Fig. 7, A and B, compare lanes 1–2 and 3–4), indicating that PBA does not modulate the levels of ER chaperones in the absence of ER stress. When N2A cells expressing HA-MC4R-GFP-I316S were treated with PBA, the drug prevented the increase of the ER chaperone GRP78 (Fig. 7, A and B, compare lanes 5–6 and 7–8). Moreover, in the cells expressing MC4R-I316S, treatment with PBA also prevented induction of CHOP (Fig. 7, C and D). This implies that treatment with PBA decreased the amount of misfolded HA-MC4R-GFP-I316S to levels that do not lead to ER stress. In conclusion, these experiments indicate that PBA increases cell surface expression of mutated MC4R by promoting folding of the receptor.

Discussion

Here we find that MC4R bearing obesity-linked mutations fail to reach the plasma membrane because the receptor misfolds in the ER and is thereby targeted for degradation. In support of this conclusion, we have several pieces of evidence. 1) As compared with the wt receptor, the four obesity-linked mutants examined here, P78L, R165W, I316S, and I317T, have increased colocalization with calnexin, an ER resident protein. This indicates that the mutated receptors are retained in the ER. The dihydrophobic motif I316 and I317 of MC4R is conserved at the C terminus of 180 different GPCRs, including all other members of the family of melanocortin receptors (16). Such a motif, preceded by a cluster of acidic residues (E308 and E315 in the MC4R sequence), has been implicated in protein sorting from the *trans*-Golgi network to

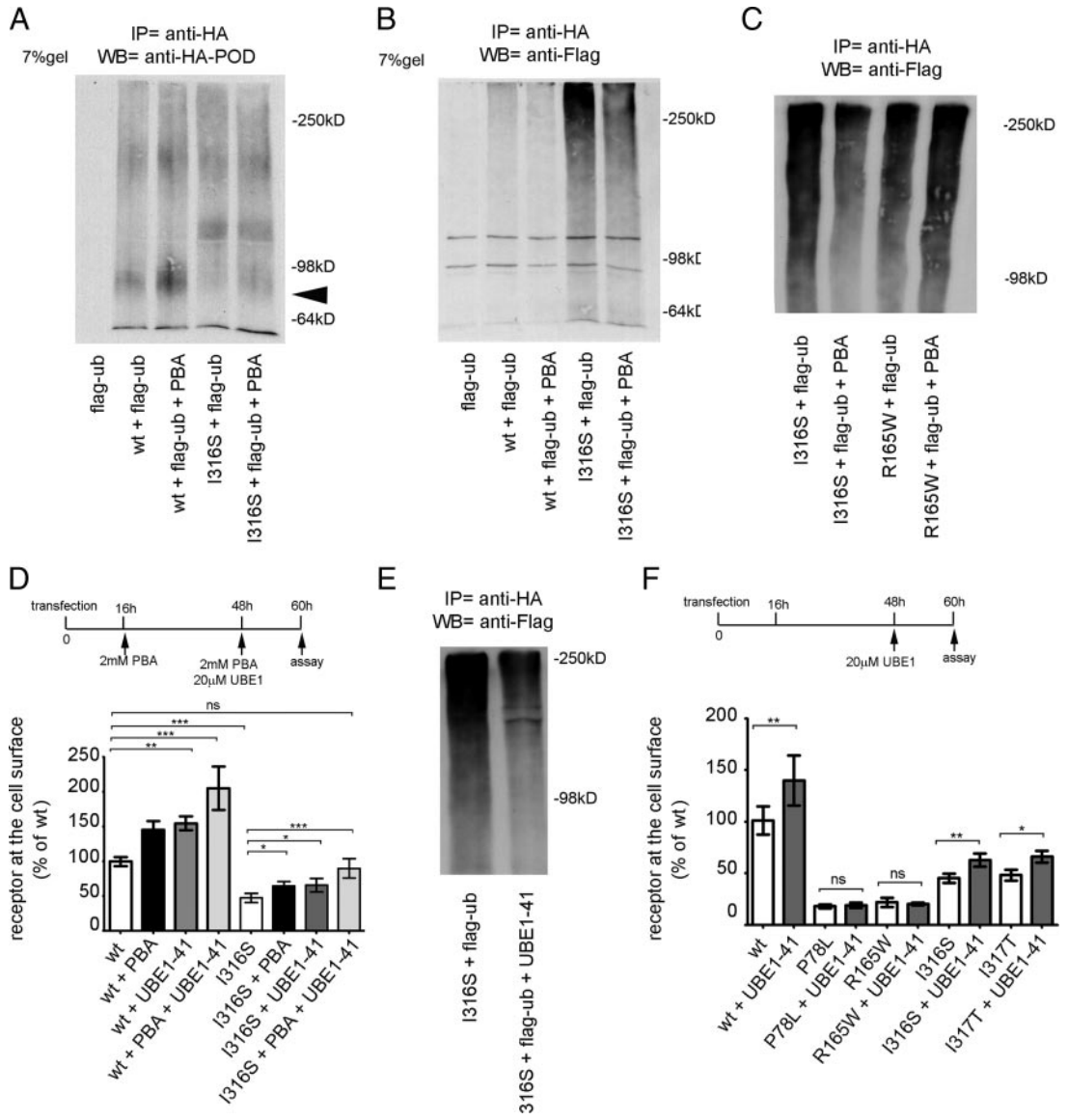

FIG. 6. PBA decreases ubiquitination of wt-HA-MC4R-GFP and mutated HA-MC4R-GFP-I316S. N2A cells were transiently transfected with Flag-ubiquitin (Flag-ub) or cotransfected with Flag-ubiquitin and wt-HA-MC4R-GFP or mutated HA-MC4R-GFP-I316S. Cells were treated with or without 2 mM PBA for 48 h as indicated. Immunoprecipitations (IP) were carried out with anti-HA antibodies, and samples were analyzed by Western blot (WB) by using POD-anti-HA antibodies (A) and mouse anti-Flag antibodies (B). *Arrowhead* indicates the band at 78 kDa. C, N2A cells were transiently cotransfected with mutated HA-MC4R-GFP-I316S or -R165W and Flag-ubiquitin and treated with vehicle alone or 2 mM PBA. Immunoprecipitations were carried out with anti-HA antibodies, and samples were analyzed by Western blot using the anti-Flag antibodies. D, N2A cells were transiently transfected with wt-HA-MC4R-GFP and mutated HA-MC4R-GFP-I316S and treated with vehicle alone or 2 mM PBA or 20 μM UBE-41 or both at the indicated time points. HA-MC4R-GFP at the cell surface was measured as in Fig. 1A and normalized to cell number using a fluorometric assay as described in *Materials and Methods*. Data are expressed as percentage of wt receptor. E, N2A cells were transiently cotransfected with mutated HA-MC4R-GFP-I316S and Flag-ubiquitin and treated with vehicle alone or 20 μM UBE-41. Immunoprecipitations were carried out with anti-HA antibodies, and samples were analyzed by Western blot by using anti-Flag antibodies. F, N2A cells were transiently transfected with wt-HA-MC4R-GFP and mutated HA-MC4R-GFP (P78L, R165W, I316S, and I317T) and treated with vehicle alone or 20 μM UBE-41 at the indicated time point. Data are expressed as in D. *, $P < 0.05$; **, $P < 0.001$; ***, $P < 0.000$; ns (nonsignificant), $P > 0.05$.

endosomes by the GGA (Golgi-localizing, γ-adaptin ear homology domain, ARF-interacting) (36, 37), which leads to the hypothesis that MC4R bearing the mutations I316S and I317T might be trapped along the trans-Golgi network/endosome route. However, our kinetic analysis of endocytosis and exocytosis of the MC4R-I316S and -I317T indicates that no traffic defects exist along this route. On the other hand, our quantitative analysis of immunofluorescence microscopy indicates that trapping in the ER was a constant feature of all obesity-linked MC4R variants under study, suggesting that the main defect of these receptors is exiting the ER. While this manuscript was being reviewed, it has been reported that another obesity-linked, intracellularly retained MC4R variant, D174W, is also localized in the ER (38), consistent with our observations. 2) MC4R-P78L, -R165W, -I316S, and -I317T exist

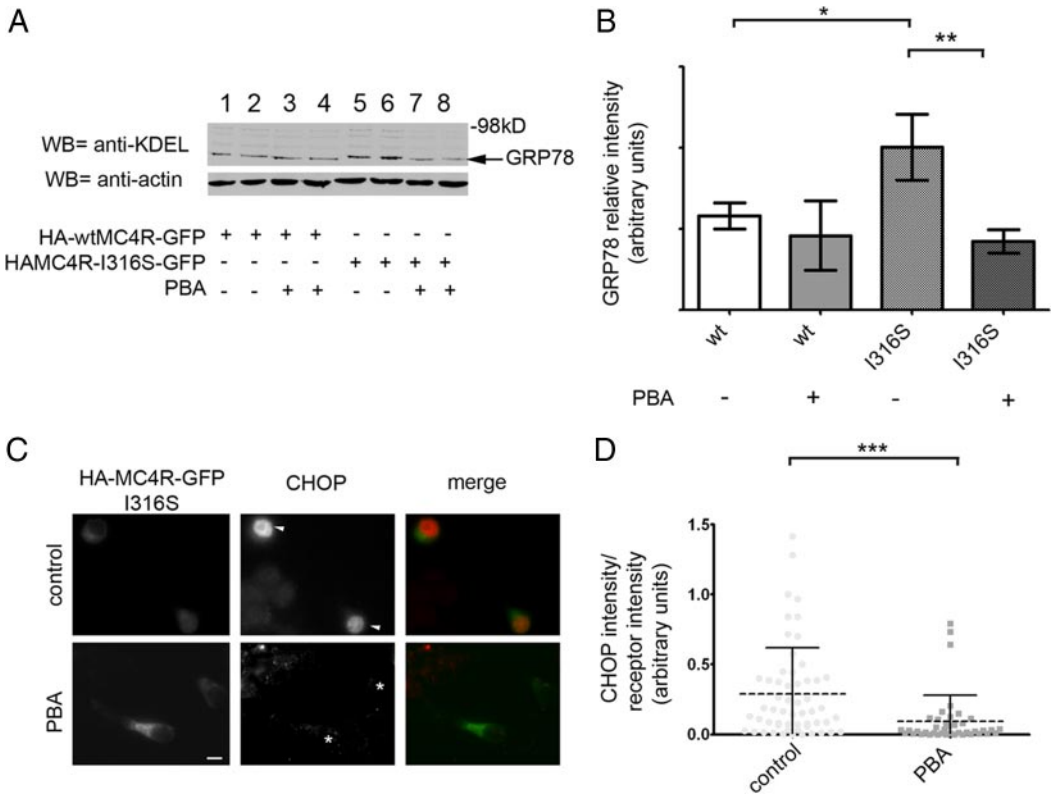

FIG. 7. PBA decreases ER stress induced by expression of mutated HA-MC4R-GFP-I316S. A, N2A cell lysates were derived from cells transfected with wt-HA-MC4R-GFP or mutated HA-MC4R-GFP-I316S. Cells were treated with vehicle alone or with 2 mM PBA for 48 h, as indicated. Cell lysates were analyzed by Western blot by the indicated antibodies. B, GRP78 and actin levels were measured by densitometry. Averages and SD were determined from three independent experiments including those shown in A. C, N2A cells were transfected with mutated HA-MC4R-GFP-I316S and treated with or without 2 mM PBA for 48 h, as indicated. Cell immunostaining was done using the primary rabbit polyclonal anti-CHOP antibodies. Secondary staining was carried out using Cy3-conjugated antirabbit antibody. D, Averages and SD of CHOP pixel intensity normalized to HA-MC4R-GFP content from cells transfected with mutated HA-MC4R-GFP-I316S and treated with vehicle alone (control, n = 56) or 2 mM PBA (PBA, n = 41). *Bar*, 25 μm. *, $P < 0.05$; **, $P < 0.001$; ***, $P < 0.0001$.

prevalently as ubiquitinated species, a yet unreported finding. In this respect, we find that most of the mutants migrate with a different pattern in SDS-PAGE with an increased fraction of the receptor existing as high molecular mass species and reduced band intensity at the predicted molecular mass of the mature receptor. Moreover, our immunoprecipitation data show that more of the MC4R bearing obesity-linked mutations than of the wt-MC4R are ubiquitinated. GPCR ubiquitination has been implicated in receptor degradation at other steps along the biosynthetic pathway (39). For example, ubiquitination is required for ligand-induced endocytosis and degradation of the GH receptor (40). However, it is unlikely that the increased ubiquitination of MC4R-I316S and -I317T functions to increase their endocytosis or routing to lysosomes because there were no changes of traffic to and from the plasma membrane of the mutants as compared with the wt receptor. 3) Expression of MC4R bearing the obesity-linked mutations and not of wt-MC4R leads to ER stress, as indicated by the increased cell levels of two chaperones, GRP78 and GRP94, which are transcriptionally regulated as part of the UPR, as well as of the proapoptotic factor CHOP.

It is well established that variants of several GPCRs linked to diseases are retained intracellularly (41), but the location and mechanism of such retention is less well understood. The great majority of mutations of V2R that cause nephrogenic diabetes insipidus fail to reach the cell surface. It has been reported that some of the disease-linked V2R mutations are trapped in the ER and others in the ER/Golgi intermediate compartment (42–44). In addition, some mutations of rhodopsin linked to autosomal dominant retinitis pigmentosa are retained in the ER, whereas others can exit the ER but are not correctly transported to the outer segments (45). Variants of MC1R, a GPCR belonging to the same family as MC4R, are associated with red hair, fair skin, and increased propensity to develop skin cancer. Some of these MC1R mutants are also retained intracellularly (46), with one, the R151C variant, trapped in the ER and another, the R160W variant, in the *cis*-Golgi (47). Interestingly, the R165W variant of MC4R, which corresponds to the R160W substitution in the MC1R protein, is retained in the ER, rather than in the *cis*-Golgi compartment. Thus, for MC4R, the main defect imposed by the R165W mutation, as for any

other disease-linked variant studied here, remains failure to fold in the ER. In the case of MC1R, disease-associated mutants generally migrated in the SDS-PAGE at the same molecular mass as the wt receptor with the exception of one variant, I155T, which migrated as multiple bands (46). Differently, in the case of MC4R, a very reproducible finding was the disappearance of the band of receptor migrating as the mature form and the increased amounts of ubiquitinated receptor present in the cell. Thus, it is possible that although many disease-associated GPCRs remain trapped intracellularly, the mechanism by which this occurs, even within members of the same family, may be different, with one possibility being that GPCR mutations lead to trafficking defects, as hypothesized for most of the MC1R disease-linked mutants (46), and another that the disease-linked mutants of GPCRs fail to fold as our results indicate to be the case for all the obesity-associated MC4R variants studied here.

Another finding of this work is that cell incubation with the chemical chaperone PBA partially rescues the cell surface expression of MC4R-I316S, -I317T, and -P78L. Functionally, this effect translates to an increased signaling with enhanced cAMP production. The mechanism by which PBA appears to function is, at least in part, by decreasing misfolding of the MC4R variants. This is indicated by the increased fraction of total MC4R-I316S that is expressed at the plasma membrane, the lower amount of ubiquitinated MC4R-I316S, and the suppression of ER stress in response to expression of the mutated receptor. PBA has also been reported to increase folding and improve secretion of mutated α-1 antitrypsin and preproparathyroid hormone (28, 29) and to improve trafficking of ΔF508-CFTR mutant from the ER to the plasma membrane (30). Different from what was observed here for the obesity-linked MC4R variants, PBA did not promote exit from the ER of other GPCR such as disease-linked rhodopsin and V2R mutants (31, 32), indicating specificity. It has been recently reported that PBA decreases ER stress in the hypothalamus of obese mice and improves leptin sensitivity, thus suggesting a potential role of PBA and other chemical chaperones in the treatment of obesity (48). The work done here suggests that, in addition to its function in leptin sensitivity, PBA may function downstream of the leptin receptor at the level of MC4R to improve cell surface expression of the receptor. In this respect, our findings suggest that, even in the absence of ER stress, PBA significantly increased the amount of wt-MC4R expressed at the plasma membrane both in the N2A cells and in the immortalized hypothalamic neurons. Because PBA reduces ubiquitination of the wt-MC4R, it is possible that the receptor has an intrinsic propensity to misfold that is at least partially corrected by the drug.

Our data indicate that PBA reduces ubiquitination of wt-MC4R and of most of the obesity-linked MC4R variants studied in this work, consistent with the concept that the drug improves folding of these receptors. We reasoned that an alternative approach to improve surface expression of MC4R was to inhibit directly ubiquitination of the receptor, thus reducing the number of MC4R molecules targeted for degradation. We find that a ubiquitin-activating enzyme inhibitor, UBE1-41, inhibited MC4R ubiquitination and improved surface expression of wt-MC4R and MC4R-I316S and I317T. Importantly, it appears that when PBA and UBE1-41 were used in combination, cell surface expression of MC4R-I316S increased to the same level as that of wt-MC4R in untreated cells. These findings are in agreement with the conclusion that misfolding and targeting for ERAD by ubiquitination is the main cause of MC4R failure to exit the ER and, thereby, of reduced expression of the receptor at the cell surface.

Interestingly, we find that PBA did not decrease the extent of MC4R-R1615W ubiquitination and did not promote cell surface expression of the receptor. Moreover, reducing MC4R-R1615W ubiquitination by UBE1-41 also did not rescue this variant to the cell surface, suggesting that the receptor is misfolded beyond repair. A study using chemical chaperones to rescue misfolded V2R mutants showed that this effect was limited to only one of nine variants (31). Thus, it appears that chemical chaperones can rescue some, but not all, of disease-linked GPCR variants trapped in the ER to the cell surface. Our observations with MC4R-I316S and MC4R-R165W suggest that those variants rescued by the inhibitor of ubiquitination are also rescued by chemical chaperones, consistent with the concept that these agents act on the same pathway.

Pharmacological chaperones are small molecules, usually peptidomimergic antagonists, which enter the cell and rescue misfolded proteins by promoting folding. In this respect, it has been proposed that pharmacological chaperones promote folding of more types of V2R mutants than chemical chaperones (31, 49). It has been recently reported that ML00253764, an inverse agonist of MC4R that can prevent body mass loss in mice (50, 51), increased plasma membrane expression of wt-MC4R and of two obesity-linked MC4R variants different from those studied here (52). However, whether ML00253764 functions to rescue MC4R by acting as a pharmacological chaperone, namely by improving folding of the receptor in the ER, rather than by acting at other steps of MC4R traffic to the plasma membrane, was not investigated. In this work, we have established that enhancing folding of wt-MC4R and of several obesity-linked MC4R variants in the ER is a critical step to control abundance of the

receptor at the cell surface of neuronal cells. Whether small molecules that bind to MC4R increase folding of the protein and whether direct inhibition of MC4R ubiquitination can be used in combination with pharmacological chaperones to further improve expression of MC4R at the plasma membrane are topics to be addressed in future studies.

It has been recently reported that in the case of prolonged ER stress, two protective branches of the UPR, IRE1 and ATF6, are attenuated, whereas PERK signaling, which induces transcription of proapoptotic factors, is maintained (25). This mechanism was mirrored in the retina of transgenic rats expressing P23H rhodopsin, another disease-linked GPCR mutant retained in the ER (25). Because sustained activation of the IRE1/XBP-1 pathway promotes cell survival in the case of prolonged ER stress, we asked whether selective activation of the XBP-1 pathway could promote MC4R-I316S folding. However, expression of XBP-1 did not resolve ER stress as indicated by the sustained levels of CHOP and did not increase the cell surface expression of the mutated receptor. This suggests that onset of the UPR is insufficient to resolve misfolding of the mutated receptor and that the mechanism by which PBA promotes folding of the receptor is different from the classical UPR. It has been recently reported that the histone deacetylase inhibitor, suberoylanilide hydroxamic acid, restores surface channel ΔF508-CFTR expression and function in human primary airway epithelia cells to levels that are 28% of those of the wt-CFTR (53). Inhibition of histone deacetylase by suberoylanilide hydroxamic acid regulates the expression of many genes involved in the folding, degradation, trafficking, cell surface stability, and function of CFTR (53). It is tempting to speculate that PBA, also possessing a histone deacetylase inhibitory effect (33), may be acting through a similar pathway to rescue expression of MC4R at the cell surface. Further studies are needed to establish the mechanism of action of PBA and identify therapeutic targets that may help the folding of the obesity-linked MC4R variants. Our observation that sustained activation of the XBP-1 pathway, an approach that nevertheless proved to relieve ER stress induced by retention of misfolded proteins (25), fails to promote MC4R folding is in striking contrast with the almost complete rescue of cell surface expression of MC4R-I316S by the combined action of PBA and inhibition of ubiquitin-activating enzyme 1. A possible conclusion is that although misfolded proteins are retained in the ER, the mechanisms of such retention seem to be different because of the specific response to agents that modulate ER homeostasis.

In summary, we find that four different obesity-linked MC4R variants, I317T, I316S, P78L, and R165W, are misfolded and retained in the ER. The onset of the UPR caused by the expression of the obesity-linked MC4R variants or specific induction of a protective branch of the UPR is not enough to counteract the misfolding of the receptor. Conversely, treatment with PBA increases the surface expression and function of obesity-linked MC4R variants by promoting folding of these proteins. In conclusion, our discoveries propose the ER folding machinery and drugs that improve folding as a main target to novel therapeutic approaches to treat some forms of hereditary obesity.

Materials and Methods

Reagents and antibodies

Lipofectamine 2000, the mouse monoclonal anti-Flag antibodies, and the nuclear dye Hoechst 33342 were purchased from Invitrogen (Carlsbad, CA). Rat monoclonal anti-HA antibody (3F10), POD-conjugated anti-HA antibody, POD-conjugated antimouse IgG, protease inhibitor (Complete Mini), and 2,2′-azino-bis(3-ethylbenzthiazoline-6-sulfonic acid (ABTS) tablets were from Roche Applied Science (Indianapolis, IN). α-MSH, 3-isobutyl-1-methylxanthine, and PBA were from Sigma-Aldrich (St. Louis, MO). POD-conjugated antirabbit IgG and POD-conjugated antigoat IgG were from Pierce Biotechnology, Inc. (Rockford, IL). Cy3-conjugated antirat, Cy5-conjugated antimouse IgG, Cy3-conjugated antirabbit IgG, and Cy5-conjugated antirabbit IgG antibodies were from Jackson ImmunoResearch (West Grove, PA). Rabbit polyclonal anti-calnexin, mouse monoclonal anti-KDEL, and cAMP ELISA kit were from Assay Designs (San Diego, CA). The rabbit polyclonal anti-CHOP antibodies were from Santa Cruz Biotechnology (Santa Cruz, CA). Mouse monoclonal anti-actin antibodies were from Chemicon International (Temecula, CA). Enhanced chemiluminescence detection kits were from PerkinElmer Life Sciences, Inc. (Boston, MA). pEGFP-N2 was from Clontech (Mountain View, CA) and XBP-1(S)-myc-ptune was from Origene (Rockville, MD). Isopropyl β-D-1-thiogalactopyranoside was purchased from Promega Corp. (Madison, WI). Hypothalamic GT1-7 cells (54, 55) were a kind gift of Dr. R. I. Weiner (University of California, San Francisco, San Francisco, CA). UBE1-41 was from Biogenova (Rockville, MD). N2A cells were a kind gift from Peter Cserjesi (Tulane University, New Orleans, LA). HEK 293 cells were purchased from the American Type Culture Collection (Manassas, VA).

Constructs

HA-MC4R-GFP and HA-MC4R plasmids were described earlier (18). The primers used to generate HA-MC4R-GFP (P78L, R165W, I316S, and I317T) mutants were 5′-AAGAACAAGAATCTGCATTCACTCATGTACTTTTTCATCTGCAGC-3′, 5′-CATAACATTATGACAGTTAAGTGGGTTGGGATCATCATAAGTTGT-3′, 5′-CTGAAGAAAACCTTCAAAGAGAGCATCTGTTGCTATCCCCTGGGA-3′, and 5′-AGGAAAACCTTCAAAGAGATCACCTGTTGCTATCCCCTGGGAGGC-3′. All mutations were confirmed by sequencing. Myc epitope (EQKLISEEDL)-tagged MC4R was generated by PCR amplification using Pfu-Turbo polymerase (Invitrogen) using MC4R-pCMV-XL4 (Origene) plasmid as template. The forward

primer, 5′-CTC AAG CTT CGA ATT CTG GCC ACC ATG **GAG CAA AAG CTG ATT TCT GAG GAG GAT** CTG GTG AAC TCC ACC CAC CGT GGG-3′, was designed with a *Hin*dIII site at the N terminus (*underlined*) and the myc epitope (in *bold*) after the starting ATG codon. The reverse primer, 5′-CGG TGG ATC CCG GGC ATA TCT GCT AGA CAA GTC ACA-3′, had a *Bam*HI site (*underlined*) at the C terminus and the MC4R stop codon (TAA) removed. Purified PCR product was digested with *Hin*dIII and *Bam*HI and then ligated into pEGFP-N2 cut with *Hin*dIII-*Bam*HI to generate a plasmid, myc-MC4R-GFP, that contains the myc-MC4R sequence upstream of, and in-frame with, the GFP coding sequence to express myc-MC4R-GFP. Plasmid DNA for transfections into mammalian cells was isolated using the DNA purification system from Promega. Flag-ubiquitin was a kind gift from Dr. JoAnn Trejo, University of North Carolina at Chapel Hill (Chapel Hill, NC).

Cell culture, transfection, and drug treatment

N2A, GT1-7, and HEK 293 cells were cultured in DMEM with 10% fetal bovine serum and penicillin/streptomycin. Cells were transiently transfected using Lipofectamine 2000 and following the manufacturer's instructions. Experiments were carried out 48 h after transfection unless indicated otherwise. For drug treatment, vehicle alone (dimethylsulfoxide) or 2 mM PBA was added 16 h after transfection and maintained until the cells were harvested. For the inhibition of ubiquitination, vehicle alone (dimethylsulfoxide) or 20 μM UBE1-41 was added 16 h before the cells were harvested.

Gel electrophoresis and immunoblotting

Separation of proteins by SDS-PAGE and immunoblotting with the indicated antibodies were performed as described (56). Unless noted otherwise, cell lysates were prepared by scraping cells from 60-mm diameter plates in 0.4 ml sample buffer containing protease inhibitors. Samples were sonicated three times for 2-sec periods and loaded onto SDS-PAGE.

Immunoprecipitations

Transfected cells grown in 60-mm dishes were scraped in immunoprecipitation buffer [100 mM Tris-HCl (pH 7.4), 50 mM NaCl, 1% Triton X-100, and protease inhibitors (Complete Mini)] and incubated for 30 min at 4 C. Cell lysates were rotated for 1 h at 4 C with the indicated antibody. After addition of protein A/G beads, the samples were further incubated for 1 h at 4 C. After three washes with immunoprecipitation buffer, the beads were resuspended in sample buffer, boiled for 5 min, and centrifuged. Supernatants and cell extracts were loaded onto a SDS-PAGE gel.

Fluorescence microscopy

Epifluorescence and confocal fluorescence images were captured with a CARV I spinning confocal imaging system (BioVision Technologies, Exton, PA) attached to an X-71 fluorescence microscope (Olympus, Tokyo, Japan). Images were collected using a CoolSNAP HQ camera (Photometrics, Tucson, AZ), and analyzed by using ImageJ software version 1.33 by Wayne Rasband (National Institutes of Health, Bethesda, MD).

Quantification of MC4R distribution by fluorescence microscopy

Fraction of total cell MC4R expressed at the cell surface

Cells were washed three times with DMEM and incubated in DMEM for 1 h at 37 C, DMEM was aspirated, and cells were transferred on ice and incubated in the same medium with rat monoclonal anti-HA antibodies for 1 h at 4 C. Cells were then fixed, washed with PBS, and incubated with PBS containing 100 μg/ml ovalbumin and Cy3-conjugated antirat antibodies without addition of detergents. Cells were then fixed with 4% formaldehyde, washed with PBS, and incubated with PBS containing 100 μg/ml ovalbumin, 0.1% Triton X-100, and Cy3-conjugated antirat antibodies.

Fraction of total cell MC4R expressed at the cell surface and endosomes

Cells were treated as above except that incubation with anti-HA was carried out for 2 h at 37 C. Cells expressing HA-MC4R-GFP were chosen at random, and the region of interest was drawn on the merged image around the compartment labeled by the HA antibodies using ImageJ software. The amount of HA-MC4R-GFP at the cell surface was estimated by dividing the fluorescence intensity of the receptor at the cell surface (Cy3) by the fluorescence intensity of the receptor in the entire cell (GFP).

Colocalization of HA-MC4R-GFP with calnexin

Immunofluorescence staining was performed as described previously (56). Confocal fluorescent images of the cells were analyzed by using ImageJ software. Briefly, after autosegmentation of calnexin fluorescence (Cy3) and HA-MC4R-GFP fluorescence (GFP), the regions of interest were analyzed by using the intensity colocalization analysis plugin in the ImageJ software, which measures the Mander's overlap coefficient M1 (57).

Quantification of KDEL and CHOP expression by immunofluorescence

Epifluorescence images of cells were obtained with constant parameters of acquisition. The region of interest was selected by manually drawing the cell margins after the GFP staining for each individual cell. Fluorescence pixel intensity in the different channels was measured by using ImageJ software.

Determination of spliced XBP-1 and ATF4 mRNA levels

Total mRNA was isolated from cells using the RNeasy Plus kit from QIAGEN (Valencia, CA). RT-PCR was carried out using the superscript one-step RT-PCR with platinum *Taq* from Invitrogen. The primers used to measure endogenous mouse XBP-1 mRNA levels were the forward 5′-TTACGGGAGAAAACTCACGGC-3′ and the reverse 5′-GGGTCCAACTTGTCCAGAATG-3′ and to measure mouse ATF4 mRNA levels were the forward 5′-TGGCGAGTGTAAGGAGCTAGAAA-3′ and the reverse 5′-TCTTCCCCCTTGCCTTACG-3′.

Quantification of HA-MC4R-GFP at the cell surface by ELISA

HA-MC4R-GFP at the cell surface by ELISA was determined as described previously (18). Briefly, N2A cells transiently transfected as indicated were washed three times with DMEM and

incubated in DMEM for 1 h at 37 C. Cells were further incubated for 1 h at 4 C in the same medium in the presence of POD-conjugated anti-HA antibodies (25 mU/ml). Cells were washed two times with ice-cold DMEM and fixed with formaldehyde at 4 C for 10 min. Cells were washed three times with PBS and POD activity was determined by using the ABTS substrate to measure the amount of receptor at the cell surface. In some experiments, where we used the potentially cell-toxic inhibitor UBE1-41, the amount of HA-MC4R-GFP at the cell surface was normalized to the number of cells used in the assay. To do that, after the quantification of HA-MC4R-GFP at the cell surface by ELISA, cells were washed twice with PBS. Cells were incubated for 20 min in PBS containing 0.2% Triton X-100 and 1 μg/ml Hoechst 33342. Cells were washed three times with PBS, and fluorescence intensity was measured by Spectra Max Gemini EM fluorimeter (Molecular Devices (Sunnyvale, CA) (excitation wavelength 350 nm, emission wavelength 461 nm). The POD activity obtained by using the ABTS substrate in each well was divided by the amount of Hoechst 33342 fluorescence in the same well. Data are expressed as percentage of wt-HA-MC4R-GFP.

Internalization of HA-MC4R-GFP by ELISA

Internalization of MC4R was monitored by ELISA as described previously (18). Briefly, N2A cells transiently transfected as indicated were washed three times with DMEM and incubated in DMEM for 1 h at 37 C. Cells were further incubated for 1 h at 4 C in the same medium in the presence of POD-conjugated anti-HA antibodies (25 mU/ml). Cells were washed two times with ice-cold DMEM and one time with DMEM at room temperature. Cells were transferred at 37 C for the indicated time intervals to allow internalization of the POD-conjugated anti-HA antibodies/HA-tagged receptor complexes. Cells were transferred on ice, washed, and fixed by incubation in PBS containing 4% paraformaldehyde at 4 C for 10 min. Cells were washed and POD activity was determined by using the ABTS substrate to measure the amount of receptor remaining at the cell surface.

Exocytosis of MC4R by ELISA

Exocytosis of MC4R was monitored by ELISA as described previously (18). Briefly, N2A cells transiently transfected as indicated were incubated with POD-conjugated anti-HA antibodies at 4 C to label all the receptor at the plasma membrane. Cells were transferred to 37 C in the continued presence of anti-HA-POD to label the pool of HA-MC4R-GFP in equilibrium with the plasma membrane. Cells were transferred on ice at different time points. Cells were fixed with 4% paraformaldehyde at 4 C for 10 min and washed, and total HA-MC4R-GFP labeled by the POD-conjugated anti-HA antibody was measured after permeabilizing cells by incubation with 0.2% Triton X-100 for 30 min. Cells were then incubated with the ABTS substrate to measure the amount of HA-MC4R-GFP labeled by anti-HA-POD.

Assay to determine cAMP

Cells were washed with DMEM and incubated with the same medium containing 0.5 mM 3-isobutyl-1-methylxanthine for 10 min and then stimulated with 100 nM α-MSH for 15 min at 37 C. The medium was aspirated, and intracellular cAMP was measured by using the immunoassay kit by Assay Designs, following the manufacturer's instructions.

Statistical analysis

Data are expressed as mean ± SD. GraphPad Prism version 5.0 (GraphPad Software, San Diego, CA) was used to perform unpaired *t* test or one-way ANOVA.

Acknowledgments

We are grateful to Dr. JoAnn Trejo (University of North Carolina at Chapel Hill) for the gift of the Flag-ubquitin plasmid and to Dr. R. I. Weiner (University of California, San Francisco) for the gift of GT1-7 cells. This paper is dedicated to the memory of Dr. Steven C. Elbein.

Address all correspondence and requests for reprints to: Giulia Baldini, Department of Biochemistry and Molecular Biology, University of Arkansas for Medical Sciences, Slot 516, 4301 West Markham, Little Rock, Arkansas 72205. E-mail: gbaldini@uams.edu.

This work was supported by the National Institutes of Health Grant R01-DK53293 and Grant R01DK080424 (to G.B.), by the Arkansas Tobacco Settlement (to G.B.), by the UAMS Interim Funding (to G.B.), and by Sturgis Research Program for Diabetes (to G.B.).

Disclosure Summary: S.G., S.M., R.R.-B., and G.B. have nothing to declare.

References

1. **Huszar D, Lynch CA, Fairchild-Huntress V, Dunmore JH, Fang Q, Berkemeier LR, Gu W, Kesterson RA, Boston BA, Cone RD, Smith FJ, Campfield LA, Burn P, Lee F** 1997 Targeted disruption of the melanocortin-4 receptor results in obesity in mice. Cell 88:131–141
2. **Vaisse C, Clement K, Durand E, Hercberg S, Guy-Grand B, Froguel P** 2000 Melanocortin-4 receptor mutations are a frequent and heterogeneous cause of morbid obesity. The Journal of clinical investigation 106:253–262
3. **Balthasar N, Dalgaard LT, Lee CE, Yu J, Funahashi H, Williams T, Ferreira M, Tang V, McGovern RA, Kenny CD, Christiansen LM, Edelstein E, Choi B, Boss O, Aschkenasi C, Zhang CY, Mountjoy K, Kishi T, Elmquist JK, Lowell BB** 2005 Divergence of melanocortin pathways in the control of food intake and energy expenditure. Cell 123:493–505
4. **Vaisse C, Clement K, Guy-Grand B, Froguel P** 1998 A frameshift mutation in human MC4R is associated with a dominant form of obesity. Nat Genet 20:113–114
5. **Yeo GS, Farooqi IS, Aminian S, Halsall DJ, Stanhope RG, O'Rahilly S** 1998 A frameshift mutation in MC4R associated with dominantly inherited human obesity. Nat Genet 20:111–112
6. **Lubrano-Berthelier C, Durand E, Dubern B, Shapiro A, Dazin P, Weill J, Ferron C, Froguel P, Vaisse C** 2003 Intracellular retention is a common characteristic of childhood obesity-associated MC4R mutations. Hum Mol Genet 12:145–153
7. **Farooqi IS, Keogh JM, Yeo GS, Lank EJ, Cheetham T, O'Rahilly S** 2003 Clinical spectrum of obesity and mutations in the melanocortin 4 receptor gene. N Engl J Med 348:1085–1095
8. **Hinney A, Schmidt A, Nottebom K, Heibült O, Becker I, Ziegler A, Gerber G, Sina M, Görg T, Mayer H, Siegfried W, Fichter M, Remschmidt H, Hebebrand J** 1999 Several mutations in the melanocortin-4 receptor gene including a nonsense and a frameshift mutation associated with dominantly inherited obesity in humans. The Journal of clinical endocrinology and metabolism 84:1483–1486

9. **Larsen LH, Echwald SM, Sorensen TI, Andersen T, Wulff BS, Pedersen O** 2005 Prevalence of mutations and functional analyses of melanocortin 4 receptor variants identified among 750 men with juvenile-onset obesity. The Journal of clinical endocrinology and metabolism 90:219–224
10. **Lubrano-Berthelier C, Cavazos M, Dubern B, Shapiro A, Stunff CL, Zhang S, Picart F, Govaerts C, Froguel P, Bougneres P, Clement K, Vaisse C** 2003 Molecular genetics of human obesity-associated MC4R mutations. Ann N Y Acad Sci 994:49–57
11. **Lubrano-Berthelier C, Dubern B, Lacorte JM, Picard F, Shapiro A, Zhang S, Bertrais S, Hercberg S, Basdevant A, Clement K, Vaisse C** 2006 Melanocortin 4 receptor mutations in a large cohort of severely obese adults: prevalence, functional classification, genotype-phenotype relationship, and lack of association with binge eating. The Journal of clinical endocrinology and metabolism 91:1811–1818
12. **Calton MA, Ersoy BA, Zhang S, Kane JP, Malloy MJ, Pullinger CR, Bromberg Y, Pennacchio LA, Dent R, McPherson R, Ahituv N, Vaisse C** 2009 Association of functionally significant Melanocortin-4 but not Melanocortin-3 receptor mutations with severe adult obesity in a large North American case-control study. Hum Mol Genet 18:1140–1147
13. **Tao YX, Segaloff DL** 2003 Functional characterization of melanocortin-4 receptor mutations associated with childhood obesity. Endocrinology 144:4544–4551
14. **Xiang Z, Litherland SA, Sorensen NB, Proneth B, Wood MS, Shaw AM, Millard WJ, Haskell-Luevano C** 2006 Pharmacological characterization of 40 human melanocortin-4 receptor polymorphisms with the endogenous proopiomelanocortin-derived agonists and the agouti-related protein (AGRP) antagonist. Biochemistry 45:7277–7288
15. **Nijenhuis WA, Garner KM, van Rozen RJ, Adan RA** 2003 Poor cell surface expression of human melanocortin-4 receptor mutations associated with obesity. J Biol Chem 278:22939–22945
16. **VanLeeuwen D, Steffey ME, Donahue C, Ho G, MacKenzie RG** 2003 Cell surface expression of the melanocortin-4 receptor is dependent on a C-terminal di-isoleucine sequence at codons 316/317. J Biol Chem 278:15935–15940
17. **Yeo GS, Lank EJ, Farooqi IS, Keogh J, Challis BG, O'Rahilly S** 2003 Mutations in the human melanocortin-4 receptor gene associated with severe familial obesity disrupts receptor function through multiple molecular mechanisms. Hum Mol Genet 12:561–574
18. **Mohammad S, Baldini G, Granell S, Narducci P, Martelli AM, Baldini G** 2007 Constitutive traffic of melanocortin-4 receptor in Neuro2A cells and immortalized hypothalamic neurons. J Biol Chem 282:4963–4974
19. **Meusser B, Hirsch C, Jarosch E, Sommer T** 2005 ERAD: the long road to destruction. Nat Cell Biol 7:766–772
20. **Marchese A, Benovic JL** 2004 Ubiquitination of G-protein-coupled receptors. Methods Mol Biol 259:299–305
21. **Kozutsumi Y, Segal M, Normington K, Gething MJ, Sambrook J** 1988 The presence of malfolded proteins in the endoplasmic reticulum signals the induction of glucose-regulated proteins. Nature 332:462–464
22. **Schröder M, Kaufman RJ** 2005 The mammalian unfolded protein response. Annu Rev Biochem 74:739–789
23. **Scheel AA, Pelham HR** 1996 Purification and characterization of the human KDEL receptor. Biochemistry 35:10203–10209
24. **Ron D, Walter P** 2007 Signal integration in the endoplasmic reticulum unfolded protein response. Nature reviews 8:519–529
25. **Lin JH, Li H, Yasumura D, Cohen HR, Zhang C, Panning B, Shokat KM, Lavail MM, Walter P** 2007 IRE1 signaling affects cell fate during the unfolded protein response. Science (New York, NY 318:944–949
26. **Calfon M, Zeng H, Urano F, Till JH, Hubbard SR, Harding HP, Clark SG, Ron D** 2002 IRE1 couples endoplasmic reticulum load to secretory capacity by processing the XBP-1 mRNA. Nature 415:92–96
27. **Sriburi R, Bommiasamy H, Buldak GL, Robbins GR, Frank M, Jackowski S, Brewer JW** 2007 Coordinate regulation of phospholipid biosynthesis and secretory pathway gene expression in XBP-1(S)-induced endoplasmic reticulum biogenesis. J Biol Chem 282:7024–7034
28. **Burrows JA, Willis LK, Perlmutter DH** 2000 Chemical chaperones mediate increased secretion of mutant alpha 1-antitrypsin (alpha 1-AT) Z: A potential pharmacological strategy for prevention of liver injury and emphysema in alpha 1-AT deficiency. Proc Natl Acad Sci USA 97:1796–1801
29. **Datta R, Waheed A, Shah GN, Sly WS** 2007 Signal sequence mutation in autosomal dominant form of hypoparathyroidism induces apoptosis that is corrected by a chemical chaperone. Proc Natl Acad Sci USA 104:19989–19994
30. **Rubenstein RC, Egan ME, Zeitlin PL** 1997 In vitro pharmacologic restoration of CFTR-mediated chloride transport with sodium 4-phenylbutyrate in cystic fibrosis epithelial cells containing delta F508-CFTR. The Journal of clinical investigation 100:2457–2465
31. **Robben JH, Sze M, Knoers NV, Deen PM** 2006 Rescue of vasopressin V2 receptor mutants by chemical chaperones: specificity and mechanism. Molecular biology of the cell 17:379–386
32. **Mendes HF, Cheetham ME** 2008 Pharmacological manipulation of gain-of-function and dominant-negative mechanisms in rhodopsin retinitis pigmentosa. Hum Mol Genet 17:3043–3054
33. **Wright JM, Zeitlin PL, Cebotaru L, Guggino SE, Guggino WB** 2004 Gene expression profile analysis of 4-phenylbutyrate treatment of IB3–1 bronchial epithelial cell line demonstrates a major influence on heat-shock proteins. Physiological genomics 16:204–211
34. **Büch TR, Heling D, Damm E, Gudermann T, Breit A** 2009 Pertussis toxin-sensitive signaling of melanocortin-4 receptors in hypothalamic GT1-7 cells defines agouti-related protein as a biased agonist. J Biol Chem 284:26411–26420
35. **Yang Y, Kitagaki J, Dai RM, Tsai YC, Lorick KL, Ludwig RL, Pierre SA, Jensen JP, Davydov IV, Oberoi P, Li CC, Kenten JH, Beutler JA, Vousden KH, Weissman AM** 2007 Inhibitors of ubiquitin-activating enzyme (E1), a new class of potential cancer therapeutics. Cancer Res 67:9472–9481
36. **Shiba T, Takatsu H, Nogi T, Matsugaki N, Kawasaki M, Igarashi N, Suzuki M, Kato R, Earnest T, Nakayama K, Wakatsuki S** 2002 Structural basis for recognition of acidic-cluster dileucine sequence by GGA1. Nature 415:937–941
37. **Robinson MS, Bonifacino JS** 2001 Adaptor-related proteins. Curr Opin Cell Biol 13:444–453
38. **Alfieri A, Pasanisi F, Salzano S, Esposito L, Martone D, Tafuri D, Daniele A, Contaldo F, Sacchetti L, Zagari A, Buono P** 2010 Functional analysis of melanocortin-4-receptor mutants identified in severely obese subjects living in Southern Italy. Gene 457:35–41
39. **Hanyaloglu AC, von Zastrow M** 2008 Regulation of GPCRs by endocytic membrane trafficking and its potential implications. Annu Rev Pharmacol Toxicol 48:537–568
40. **Strous GJ, van Kerkhof P, Govers R, Ciechanover A, Schwartz AL** 1996 The ubiquitin conjugation system is required for ligand-induced endocytosis and degradation of the growth hormone receptor. EMBO J 15:3806–3812
41. **Conn PM, Ulloa-Aguirre A, Ito J, Janovick JA** 2007 G protein-coupled receptor trafficking in health and disease: lessons learned to prepare for therapeutic mutant rescue in vivo. Pharmacol Rev 59:225–250
42. **Hermosilla R, Oueslati M, Donalies U, Schonenberger E, Krause E, Oksche A, Rosenthal W, Schulein R** 2004 Disease-causing V(2) vasopressin receptors are retained in different compartments of the early secretory pathway. Traffic (Copenhagen, Denmark) 5:993–1005
43. **Robben JH, Sze M, Knoers NV, Deen PM** 2007 Functional rescue of vasopressin V2 receptor mutants in MDCK cells by pharmacochaperones: relevance to therapy of nephrogenic diabetes insipidus. Am J Physiol 292:F253–F260
44. **Los EL, Deen PM, Robben JH** 2010 Potential of non-peptide

(ant)agonists to rescue vasopressin V2 receptor mutants for the treatment of X-linked nephrogenic diabetes insipidus. J Neuroendocrinol 22:393–399
45. **Mendes HF, van der Spuy J, Chapple JP, Cheetham ME** 2005 Mechanisms of cell death in rhodopsin retinitis pigmentosa: implications for therapy. Trends Mol Med 11:177–185
46. **Beaumont KA, Newton RA, Smit DJ, Leonard JH, Stow JL, Sturm RA** 2005 Altered cell surface expression of human MC1R variant receptor alleles associated with red hair and skin cancer risk. Hum Mol Genet 14:2145–2154
47. **Sánchez-Laorden BL, Herraiz C, Valencia JC, Hearing VJ, Jiménez-Cervantes C, Garcia-Borrón JC** 2009 Aberrant trafficking of human melanocortin 1 receptor variants associated with red hair and skin cancer: Steady-state retention of mutant forms in the proximal golgi. J Cell Physiol 220:640–654
48. **Ozcan L, Ergin AS, Lu A, Chung J, Sarkar S, Nie D, Myers Jr MG, Ozcan U** 2009 Endoplasmic reticulum stress plays a central role in development of leptin resistance. Cell Metab 9:35–51
49. **Morello JP, Salahpour A, Laperrière A, Bernier V, Arthus MF, Lonergan M, Petäjä-Repo U, Angers S, Morin D, Bichet DG, Bouvier M** 2000 Pharmacological chaperones rescue cell-surface expression and function of misfolded V2 vasopressin receptor mutants. J Clin Invest 105:887–895
50. **Nicholson JR, Kohler G, Schaerer F, Senn C, Weyermann P, Hofbauer KG** 2006 Peripheral administration of a melanocortin 4-receptor inverse agonist prevents loss of lean body mass in tumor-bearing mice. The Journal of pharmacology and experimental therapeutics 317:771–777
51. **Vos TJ, Caracoti A, Che JL, Dai M, Farrer CA, Forsyth NE, Drabic SV, Horlick RA, Lamppu D, Yowe DL, Balani S, Li P, Zeng H, Joseph IB, Rodriguez LE, Maguire MP, Patane MA, Claiborne CF** 2004 Identification of 2-[2-[2-(5-bromo-2-methoxyphenyl)-ethyl]-3-fluorophenyl]-4,5-dihydro-1H-imidazole (ML00253764), a small molecule melanocortin 4 receptor antagonist that effectively reduces tumor-induced weight loss in a mouse model. J Med Chem 47:1602–1604
52. **Fan ZC, Tao YX** 2009 Functional characterization and pharmacological rescue of melanocortin-4 receptor mutations identified from obese patients. J Cell Mol Med 13:3268–3282
53. **Hutt DM, Herman D, Rodrigues AP, Noel S, Pilewski JM, Matteson J, Hoch B, Kellner W, Kelly JW, Schmidt A, Thomas PJ, Matsumura Y, Skach WR, Gentzsch M, Riordan JR, Sorscher EJ, Okiyoneda T, Yates JR, 3rd, Lukacs GL, Frizzell RA, Manning G, Gottesfeld JM, Balch WE** 2010 Reduced histone deacetylase 7 activity restores function to misfolded CFTR in cystic fibrosis. Nat Chem Biol 6:25–33
54. **Weiner RI, Wetsel W, Goldsmith P, Martinez de la Escalera G, Windle J, Padula C, Choi A, Negro-Vilar A, Mellon P** 1992 Gonadotropin-releasing hormone neuronal cell lines. Front Neuroendocrinol 13:95–119
55. **Mellon PL, Windle JJ, Goldsmith PC, Padula CA, Roberts JL, Weiner RI** 1990 Immortalization of hypothalamic GnRH neurons by genetically targeted tumorigenesis. Neuron 5:1–10.
56. **Granell S, Baldini G, Mohammad S, Nicolin V, Narducci P, Storrie B, Baldini G** 2008 Sequestration of mutated α1-antitrypsin into inclusion bodies is a cell-protective mechanism to maintain endoplasmic reticulum function. Mol Biol Cell 19:572–586
57. **Manders EM, Stap J, Brakenhoff GJ, van Driel R, Aten JA** 1992 Dynamics of three-dimensional replication patterns during the S-phase, analysed by double labelling of DNA and confocal microscopy. J Cell Sci 103 (Pt 3):857–862